

## REVISITING THE CONCEPT OF HTR WALLPAPER FUEL

**Alain Marmier**  
**Michael A. Fütterer**  
**Kamil Tuček**  
European Commission  
Joint Research Centre  
Institute for Energy  
Petten, The Netherlands

**Han de Haas**  
**Jim C. Kuijper**  
Nuclear Research and consultancy Group  
Petten, The Netherlands

**Jan Leen Kloosterman**  
Delft University of Technology  
Faculty of Applied Sciences  
Physics of Nuclear Reactors  
Delft, The Netherlands

### ABSTRACT

Good safety characteristics are an outstanding feature of High Temperature Reactors (HTR):

- The high graphite inventory in the core provides significant thermal inertia. Graphite also has a high thermal conductivity, which facilitates the transfer of heat to the reflector, and it can withstand high temperatures.
- The strongly negative Doppler coefficient gives a negative feedback, such that the reactor shuts down by itself in overpower accidental conditions.
- The high quality of fuel elements – tri-isotropic (TRISO) coated particles – minimizes operational and accidental fission gas release. The materials selected have resistance to high temperatures.
- The low power density enables stabilization of core temperature significantly below the maximum allowable, even in case of severe accidents (such as loss-of-coolant accident).

Together, these aspects significantly reduce the risk of massive fission product release, which is one of the attractive features of HTRs.

The fuel that is currently used in pebble bed reactors such as AVR, HTR-10 and soon PBMR is based on a homogeneous distribution of coated particles within a fuel pebble. This homogenizes power density in the pebble, but creates a radial temperature gradient across the fuel sphere. Fuel particles placed at its centre has the highest temperature. Reducing the average temperature of particles would help preserve their integrity and maintain the resistance of the first barrier against fission product release.

As early as the 1970s, attempts were made to reduce the peak fuel temperature by means of so-called “wallpaper fuel”, in which the fuel is arranged in a spherical shell within a pebble. At that time, the production process was not sufficiently mature and had caused unacceptable damage to the (less performing) BISO particles, which is why this fundamentally promising concept was

abandoned. In this paper, proposals will be put forward to improve the production process.

This paper further exploits the wallpaper concept, not only from the point of view of temperature reduction, but also for enhanced neutronic performance through improved neutron economy, resulting in reduced fissile material and/or enrichment needs or providing the potential to achieve higher burn-up. Parameters modified were the density of the central fuel-free graphite zone and the packing fraction of the fuel zone.

It is demonstrated that this fuel type impacts positively on the fuel cycle, reduces production of minor actinides (MA) and improves the safety-relevant parameters of the reactor. A comparison of these characteristics with PBMR-type fuel is presented. The calculations were performed using Monte Carlo neutron transport and depletion codes MCNP/MCB and the deterministic code WIMS.

By comparison with PBMR fuel, the “wallpaper design” of the fuel pebble results in an effective neutron multiplication coefficient increase (by about 2%), which is combined with a decrease of between 3 and 15% in MA production. An improved neutron economy of the heterogeneous design enables enrichment of the “wallpaper type” of fuel to be reduced by more than 6%.

### INTRODUCTION

Invented by Professor Dr. Rudolf Schulten [1] in the 1950s and developed in Germany in the 1970s, High Temperature Reactors feature several important inherent and passive safety characteristics, namely:

- high thermal inertia,
- negative Doppler coefficient,
- high quality fuel,
- low power density.

Together, the aforementioned aspects prevent massive release of fission products in the case of an accident and core melt down.

Other key beneficial features of the HTR are its high thermal efficiency, its high outlet temperature, suitable for process heat production [2] and its versatile fuel cycles (high burn-up and MA management) [3]. The abovementioned aspects make this concept suitable for advanced applications, in conformity with the Generation IV International Forum objectives of sustainability. However, it should be noted that HTRs do not breed in U-Pu cycle, and MA transmutation would most probably require the creation of fast zones in HTRs.

Since this reactor design has been investigated over at least three decades, the concept is mature and generates international interest: China and South Africa are heavily involved in the development of their own HTR technology. In both cases, the fuel is based on a homogeneous distribution of coated particles within a fuel pebble. This homogenizes power distribution, leading to a radial temperature gradient across the fuel sphere. Particles placed in its centre have the highest. Reducing the temperatures of TRISO particles would preserve their integrity and thus maintain the resistance of the first barrier against fission product release.

Already in the 1970s [4], attempts were made to reduce the peak fuel temperature by so-called “wallpaper fuel”, in which the fuel is arranged in a spherical shell within a pebble. At that time, the production process was not sufficiently mature and had caused unacceptable damage to the (less performing) BISO particles: Under irradiation conditions in the DRAGON reactor, the severe shrinkage of carbon (coke) - used as a synthetic resin to bind particles - tore off the outer PyC layer of particles. For this reason, this fundamentally promising concept has been discarded [1]. As particle and pebble production processes have improved since the 1970s, this issue should now be resolved.

This paper further exploits the “wallpaper concept”, not only with a view to temperature reduction but also for enhanced neutronic performance through improvement of the neutron economy, allowing reduction of enrichment needs and fissile material inventories, and possibly achieving higher burn-up. Parameters optimized in the analyses were the particle packing fraction and the density of the central fuel-free graphite. The use of graphite with higher density ( $2.1 \text{ g/cm}^3$ ) was investigated, as this design change improves neutron economy as well as thermal inertia of the reactor, resulting in a lower peak temperature in the event of a depressurized loss-of-coolant accident.

This paper also describes the method used to determine the temperature profile across the pebble, averaged fuel temperature and also temperature gradient – the latter being a decisive factor in promoting kernel migration [5]. Finally, this paper puts forward a proposal to enable the production process of this fuel.

### RE-VISITING “WALLPAPER” FUEL

A wallpaper fuel was originally developed by Teuchert [4] in the 1970s to lower particle temperatures. By locating particles in a spherical shell, close to the surface of the pebble, the temperature profile was flattened and the peak temperature reduced.

This approach avoids positioning fuel particles in the central part of the pebble, where the temperature is highest. This lowers

both peak and average temperatures of fuel particles, decreasing the probability of failure and fission gas release.

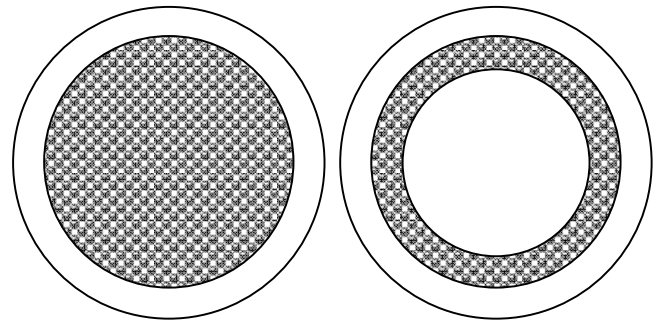


Figure 1: Classic and “wallpaper design” of HTR pebbles

Since the particle packing fraction of a PBMR pebble is relatively low compared to HTR compacts [6] (8.9% vs. 30% for the compacts), condensing them within a layered fuel zone is thought feasible and would create a central fuel-free zone. Assuming a 30% packing fraction applied to a pebble, the maximum radius of this central fuel free zone can be estimated at 2.22 cm.

### METHOD

#### Design specifications of the different pebbles investigated

In addition to the modification brought about by the wallpaper fuel, increasing the density of the central fuel free zone offers the possibility of designing an even more thermal HTR. In PBMR pebbles, the matrix graphite density ( $1.75 \text{ g/cm}^3$ ) is limited by other constraints imposed on the material - it is supposed to fix particles, remove their power and also exhibit good isotropy. The latter characteristic is important and has to be maintained in order to avoid temperature gradient-induced stress formations in the pebble during its lifetime. Alleviating the thermal issue (power peaking) allows graphite with a higher density, for instance up to  $2.1 \text{ g/cm}^3$ , to be considered, as described in [7].

Finally, since modifications suggested so far (fuel-free central zone, higher graphite density) are intended to improve the neutronics of the reactor, it would also be possible to decrease fuel enrichment as a means of compensation, i.e. design a wallpaper pebble with reduced enrichment. This would have beneficial impacts on fuel costs (manufacturing), fissile material requirements.

Table 1 presents the characteristics of the four pebbles compared throughout this study and depicted in Figure 2.

Fuel type	PBMR	Wallpaper Variant 1	Wallpaper Variant 2	Wallpaper Variant 3
Number of particles	14365	14365	14365	14365
Enrichment [ $^{235}\text{U}$ wt.%]	9.6%	9.6%	9.6%	9.0%
Graphite density [ $\text{g/cm}^3$ ]	1.75	1.75	2.1	2.1
Particle packing fraction	8.95%	30%	30%	30%

Table 1: Characteristics of the four pebbles investigated

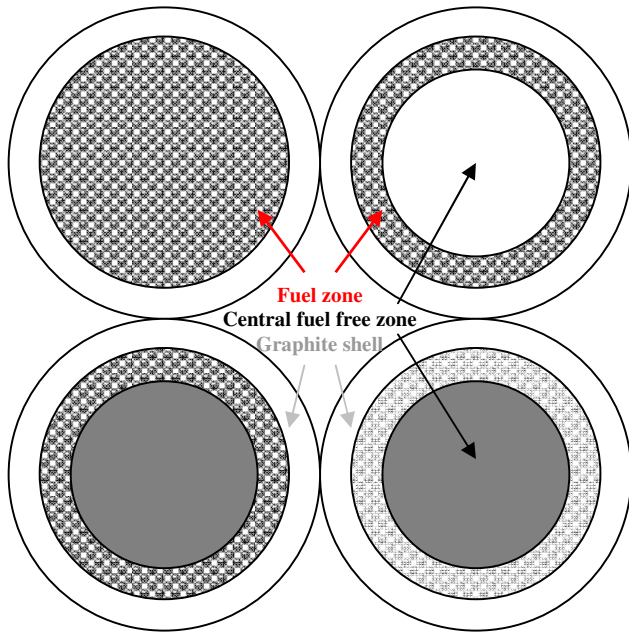


Figure 2: PBMR (top left) variant 1 (top right),  
variant 2 (bottom left) variant 3 (bottom right)

### Description of computational tools

Besides a gain in temperature, modifications also have a significant impact on core neutronics: For this reason, the four pebbles specified in Figure 2 were compared in full core simulations to determine the effects of fuel modifications on reactivity, spent fuel composition and the safety features of the reactor. Comparison between the PBMR pebble and variant 1 allow conclusions to be drawn regarding the impact of creation of the fuel free zone, between variant 1 and 2 regarding the increase of graphite density and between variant 2 and 3 concerning the influence of fuel enrichment.

The core model of the MCNP/MCB simulations – that were used for first estimate of neutron multiplication and spent fuel composition – was significantly simplified. Only the pebble bed, composed of fresh fuel, surrounded by pure graphite reflectors was modelled. MCB [8] is a general-purpose Monte Carlo Continuous-Energy Burn-up code used to calculate evolution of nuclide density over time with burn-up or decay.

The code integrates MCNP, version 4C, [9] which is used to calculate neutron transport, and a novel Transmutation Trajectory Analysis code (TTA), which is used for calculating density evolution, including formation and analysis of the transmutation chain. Thus, it includes eigenvalue calculations of critical and sub critical-systems, as well as neutron transport calculations in fixed source mode or k-code mode to obtain the reaction rates and energy deposition that are necessary for calculating burn up. MCB is compatible with MCNP and preserves its structure: Complete burn-up calculations can be made in one single run, involving minor modifications to an MCNP input file.

The PANTHERMIX [10] code system, developed at NRG, performs core physics analyses on HTRs. Based on the WIMS lattice code, the 3-D steady-state and transient core physics code PANTHER (Serco Assurance, UK) and the 2-D R-Z HTR

thermal hydraulics code THERMIX-DIREKT (Research Centre FZJ Jülich, Germany), PANTHERMIX enables, among others, characterization of core during steady-state operation (determination of the equilibrium core of a continuous reload pebble bed reactor) and transients (De/Pressurized Loss of Forced Cooling Accidents). The core model used throughout this study corresponds to the PBMR 400MW as defined in the “OECD 400MW benchmark” [11].

### Description of the approach

Several modifications to core neutronics are expected. They are due to different phenomena:

- HTRs, with stochastic particle distribution within pebbles and pebbles within the core, are presented as heterogeneous. By packing particles in a thinner fuel layer, heterogeneities are enhanced, which decreases the probability of resonance absorption.
- Graphite density increase tends to modify the moderator-to-fuel ratio. This impacts on the neutron spectrum: A spectral shift towards thermal energy is expected.
- Raising the particle packing fraction within a smaller fuel zone should improve the Dancoff factor. This should raise the neutron resonance escape probability, also contributing to reactivity increase.

In order to understand the different phenomena, reaction rates were calculated for the different energy groups (boundaries of 0 – 0.625 – 6.74E4 – 1.35E6 – 1.96E7 eV for the thermal to fast groups respectively).

### RESULTS OF FULL CORE SIMULATIONS

#### Criticality and the six factor formula

The effective neutron multiplication factor can be defined as the product of the six following parameters [12]:

- $\eta$  is the average number of neutrons produced for every thermal neutron absorbed in the fuel,
- $f$  represents the thermal utilization of the reactor,
- $\epsilon$  is the fast fission factor,
- $p$  stands for the resonance escape probability,
- $p_{FNL}$  and  $p_{TNL}$  are the probabilities that a fast/thermal neutron will not leak out of the system.

Table 2 summarizes the characteristics of the four pebbles tested and the results of the MCNP simulations for the determination of the six factor formula.

Fuel type	PBMR	Variant 1	Variant 2	Variant 3
$\eta$	1.9749	1.9748	1.9749	1.9693
$f$	0.8695	0.8699	0.8720	0.8679
$\epsilon$	1.1003	1.1005	1.0956	1.0909
$p$	0.7441	0.7477	0.7558	0.7583
$p_{NL}$	0.9336	0.9335	0.9362	0.9349
$k_{eff}$ tally	<b>1.313</b>	<b>1.320</b>	<b>1.336</b>	<b>1.322</b>
$k_{eff}$ track length	<b>1.314</b>	<b>1.320</b>	<b>1.335</b>	<b>1.322</b>

Table 2: Six factor formula and criticality calculated in MCNP

By means of MCNP calculation,  $p_{NL} = p_{FNL} * p_{TNL}$  is directly available, while  $\eta$ ,  $f$ ,  $\epsilon$  and  $p$  require tallies and multipliers.

The first observation is the good correlation between the neutron multiplication factor determined by the six factor formula ( $k_{eff}$  tally) and the corresponding MCNP value ( $k_{eff}$  track length). This, coupled with the high precision of the calculation and the intrinsic characteristic of the MCNP code (more suitable for comparative studies than for determination of accurate results), provides high confidence in the six factor values and enable the following interpretations to be made. From Table 2, we observe that the increase in  $k_{eff}$  is about 1700 pcm. This is due to the mutual interplay of several effects:

- $\eta$  is impacted by the enrichment decrease, which obviously decreases neutron production.
- $f$  denotes the competition between neutron absorption in the fuel and other materials. The value is increased by the creation of the fuel free zone (heterogeneities) and the higher graphite density (moderation increase), while a fuel enrichment drop reduces  $f$  (related to the predominant impact of fuel absorption on  $f$ ). However, the changes are small and within the standard deviation of our Monte Carlo calculations.
- If  $\epsilon$  is raised slightly by the creation of a fuel free zone (higher average neutron energy), it falls with higher graphite density or lower enrichment (moderation).
- $p$  is increased throughout these comparisons due to heterogeneities (from the creation of a fuel free zone and its density increase) and a decrease in enrichment. This can be linked to the decrease of parasitic capture in  $^{235}\text{U}$ , which is not fully offset by an increase of parasitic capture in  $^{238}\text{U}$  in the region above 0.625 eV (cf. Table 5).
- Variations of  $p_{NL}$  are related to the fast neutron flux, which is the main cause of leakage (cf. Table 4).

Several phenomena account for the effects displayed here:

### Heterogeneities

Heterogeneity (separation of moderator/coolant and fuel) improves neutron economy in the reactor [13]. Due to heterogeneity between fuel and moderator zones, there is a higher probability for a neutron to be moderated before entering a second fuel zone, where it has a higher probability of producing fission (i.e. the probability for neutron capture in the resonance region of  $^{238}\text{U}$  decreases).

Owing to the wallpaper design of the fuel pebble, neutron economy in the reactor is improved, which also results in higher neutron multiplication. Heterogeneity reduces the neutron capture probability  $p$  and neutrons are therefore further moderated (cf.  $\epsilon$  in Table 2).

### Moderator/Fuel ratio

According to [12] the ratio of moderator volume to fuel volume in a fuel cell characterizes the effectiveness of neutron moderation in the core. This is true for homogenized lattice cells. For heterogeneous fuel cells, account also has to be taken of spatial distribution, as shown by the comparison between PBMR fuel and variant 1 in Table 3.

Fuel type	PBMR	Variant 1	Variant 2	Variant 3
$k_{eff}$ at 0s [-]	1.313	1.321	1.336	1.322
$\sigma$	0.065%	0.073%	0.055%	0.068%
Fraction of $^{12}\text{C}/^{235}\text{U}$ in fuel [-]	1.82E+02	1.82E+02	2.00E+02	2.14E+02

Table 3: Semi-correlation of criticality and moderator/fuel ratio

Pebbles are deliberately designed to be under-moderated: Due to fuel depletion, moderation increases, somehow compensating for fission product poisoning. By raising the fuel free zone graphite density, the moderator-to-fuel mass ratio in a fuel cell is also raised, improving neutron multiplication (cf. comparison between variants 1 and 2 in Table 3).

### Neutron spectrum modification

As a result of geometry and materials modifications, the neutron flux also changes. Table 4 displays the neutron flux in TRISO particles averaged over the core.

Fuel type	PBMR	Variant 1	Variant 2	Variant 3
<b>Energy group</b>	<b>Averaged neutron flux on kernels [<math>\text{n} \cdot \text{cm}^{-2} \cdot \text{s}^{-1}</math>]</b>			
Thermal	5.770E+13	5.773E+13	5.787E+13	6.181E+13
Lower epithermal	5.765E+13	5.763E+13	5.459E+13	5.534E+13
Higher epithermal	2.253E+13	2.259E+13	2.111E+13	2.133E+13
Fast	8.049E+12	8.148E+12	7.654E+12	7.740E+12
Total	1.459E+14	1.461E+14	1.412E+14	1.462E+14

Table 4: Neutron fluxes for the pebble design variants

Between PBMR fuel and variant 1, the change in the thermal spectra is  $3.5 \cdot 10^{10} / \text{cm}^2 / \text{s}$ , while in the fast range it is  $10.7 \cdot 10^{10} / \text{cm}^2 / \text{s}$ . Due to much larger cross-sections in the thermal range, the effect of the former is dominant and means increased  $\eta$ . Note a decrease of spectrum in the energy range of 0.625 - 6.74E4 eV which, together with higher  $p$  values, indicates enhanced down-scattering of neutrons in graphite to energies below pronounced  $^{238}\text{U}$  resonances.

To further exemplify the spectral shift to thermal energy, Table 5 presents energy dependent reaction rates and the averaged neutron energy.

Fuel type	PBMR	Variant 1	Variant 2	Variant 3
<b>Energy group</b>	<b>Fission rate <math>\text{UO}_2</math> [<math>\text{fis} \cdot \text{particle}^{-1} \cdot \text{s}^{-1}</math>]</b>			
Thermal	1.93E+09	1.93E+09	1.94E+09	1.95E+09
Lower epithermal	1.82E+08	1.82E+08	1.74E+08	1.66E+08
Higher epithermal	4.70E+06	4.71E+06	4.40E+06	4.18E+06
Fast	7.11E+08	7.21E+08	6.77E+08	6.79E+08
Total	2.13E+09	2.13E+09	2.13E+09	2.13E+09
<b>Energy group</b>	<b>Capture rate <math>\text{UO}_2</math> [<math>\text{abs} \cdot \text{particle}^{-1} \cdot \text{s}^{-1}</math>]</b>			
Thermal	4.52E+08	4.52E+08	4.54E+08	4.63E+08
Lower epithermal	7.25E+08	7.06E+08	6.78E+08	6.84E+08
Higher epithermal	5.18E+06	5.19E+06	4.85E+06	4.88E+06
Fast	8.29E+05	8.39E+05	7.90E+05	7.96E+05
Total	1.18E+09	1.16E+09	1.14E+09	1.15E+09
<b>ANE [MeV]</b>	<b>1.84E-04</b>	<b>1.85E-04</b>	<b>1.73E-04</b>	<b>1.64E-04</b>

Table 5:  $\text{UO}_2$  reaction rates and average neutron energy

As expected,  $p$  is influenced by the decrease in the capture cross-section, while  $\epsilon$  follows the trend of the averaged neutron energy. Both are increased by the creation of the fuel-free zone, and decrease when graphite density is raised. The use of denser graphite means even more thermalised spectrum than in variant 1, which decreases  $^{238}\text{U}$  capture rate and MA build-up even further.

Finally, a drop in enrichment reduces neutron absorption leading to fission of  $^{235}\text{U}$  ( $\eta$ ). This change raises all parts of the spectrum, but with a higher impact on the thermal part. This thermal shift confirms the higher moderation achieved by neutrons, although this is also accompanied by a higher  $^{238}\text{U}$  capture rate, which leads to higher MA build-up.

### Dancoff factor

Besides the neutron spectrum, heterogeneity also influences the Dancoff factors. The switch from PBMR to wallpaper fuel requires a modification of geometry, i.e. particles are packed more densely in a shell layer. This increases the probability of a neutron to jump from one kernel to another without interactions in-between with the moderator. The Dancoff factor is actually two separate factors [14]:

- The intra-pebble Dancoff factor (or Dancoff factor of an infinite number of fuel particles) is calculated and corrected for the probability that neutrons may leak from the fuel zone of a pebble to the moderator shell without interaction.
- The inter-pebble Dancoff factor takes into account the probability that these escaping neutrons may enter a fuel kernel in another pebble, either a neighbouring one or one that is further away.

Since the diameter of the central fuel-free zone is the order of magnitude of one neutron mean free path in graphite, the use of a wallpaper fuel increases the intra-pebble Dancoff factor. The same applies to the inter-pebble Dancoff factor, as the fuel zones of two adjacent pebbles are closer. The Dancoff factors, calculated with PEBDAN [14], are available in Table 6:

PBMR	Variant 1	Variant 2
0.420	0.589	0.590

Table 6: Dancoff factor for PBMR and wallpaper fuels calculated with PEBDAN

As an increase in the Dancoff factor is related to an increase in the resonance escape probability (cf.  $p$  in Table 2), this leads to increased neutron multiplication. This fact is corroborated by a decrease in the lower epithermal flux, indicating higher fuel self-shielding (Table 4).

### Fuel burn-up

Table 7 displays fuel burn-up characteristics, including production/destruction rates of actinide isotopes. The length of the fuel cycle was 360 days; reactor power was 400 MWth.

When considering  $^{240}\text{Pu}$  (non-fissionable), it can be seen that heterogeneity reduces MA build-up, while lower enrichment increases it. This suggests that modifications introduced by variants 1 and 2 improve the core as a burner, while variant 3 improves its breeding capacity.

$k_{\text{eff}}$ at 360d [-]	1.107	1.115	1.129	1.115
$\sigma$	0.062%	0.065%	0.058%	0.064%
$^{235}\text{U}$ cons.	1.10E+05	1.10E+05	1.10E+05	1.08E+05
$^{239}\text{Pu}$ prod.	2.41E+04	2.36E+04	2.27E+04	2.27E+04
$^{240}\text{Pu}$ prod.	9.76E+03	9.51E+03	9.30E+03	9.82E+03
$^{241}\text{Pu}$ prod.	5.34E+03	5.24E+03	4.97E+03	5.41E+03
$^{241}\text{Am}$ prod.	4.93E+01	4.83E+01	4.58E+01	4.91E+01

Table 7: Fuel composition evolution through burn-up [ $\text{g}^*\text{TWh}_{\text{th}}^{-1}$ ]

This is further underlined by the decrease in  $^{235}\text{U}$  consumption, due to its lower initial enrichment and is compensated for by a larger total production of Pu. The evidence for this is a lower  $^{239}\text{Pu}$  concentration, but higher  $^{241}\text{Pu}$  and  $^{241}\text{Am}$  concentrations (compared to variant 1). In fact, in variant 3 only 55.9 % of total power at the end of life is due to fission of  $^{235}\text{U}$ , while the corresponding figure for variant 1 is higher, at 57.1%. Table 8 shows the distribution of fission power between major fissile isotopes for each fuel variant after fuel ageing.

Fuel type	PBMR	Variant 1	Variant 2	Variant 3
%FP $^{235}\text{U}$ [-]	57.11%	57.66%	58.52%	55.85%
%FP $^{238}\text{U}$ [-]	0.35%	0.35%	0.32%	0.33%
%FP $^{239}\text{Pu}$ [-]	35.97%	35.47%	34.86%	36.60%
%FP $^{241}\text{Pu}$ [-]	6.55%	6.48%	6.25%	7.18%

Table 8: Fission power from major fissile isotopes

The conversion ratio for the different fuel loading was calculated by checking the fuel inventory in thermal fissile minor actinides ( $^{233}\text{U}$ ,  $^{235}\text{U}$ ,  $^{239}\text{Pu}$  and  $^{241}\text{Pu}$ ) before and after the irradiation period (Table 9).

Fuel type	PBMR	Variant 1	Variant 2	Variant 3
CR at 360d [-]	0.682	0.680	0.678	0.663

Table 9: Conversion ratio for the different fuel loadings

This confirms that it is possible to design an even more efficient burner: By modifying the geometry or the material of the pebble, the conversion ratio drops. This is even more efficient when fuel enrichment is decreased, although increasing MA production.

### Temperature coefficient of reactivity

The Doppler effect contributes to the inherent safety of all reactors, but this assertion is even more valid for HTRs. In HTRs, a negative reactivity feedback, introduced by a broadening of neutron absorption resonances following temperature excursion, can induce a reactor to save shut-down (simulation of the loss of coolant accident with the AVR reactor [1] and transient tests at the HTR-10 reactor [15]). The Doppler feedback can be estimated by simulating the same reactor and fuel at different temperatures and studying the resulting variations in  $k_{\text{eff}}$ .

Table 10 displays the effective neutron multiplication coefficient calculated in MCNP (1  $\sigma$  standard deviation below 1.4%) and the fuel temperature coefficient of reactivity CTF.

Fuel type	PBMR	Variant 1	Variant 2	Variant 3
$k_{\text{eff}}$ at 300 K	1.368	1.374	1.388	1.374
$k_{\text{eff}}$ at 1800 K	1.289	1.297	1.313	1.300
$CT_F$ [pcm/K]	-2.96	-2.85	-2.74	-2.78

Table 10: Criticality vs. fuel temperature and  $CT_F$

$CT_F$  was calculated with  $k_{\text{eff}}$  values corresponding to the change of fuel temperature (not density) from 300 to 1800 K using the formula from [12]:

$$CT_F = \frac{\Delta \rho}{\Delta T}$$

The drop in  $CT_F$  between PBMR fuel, variants 1 and 2 is caused by higher moderation: Table 5 displays the averaged neutron energy in MeV. This reveals a spectral shift to thermal energies, which decreases the neutrons available for absorption in the resonance range. The increase between variants 2 and 3 is a direct result of the increase in  $^{238}\text{U}$  concentration (or decrease in  $^{235}\text{U}$  enrichment).

A similar trend is observed when raising the graphite temperature (cf. Table 11).

Fuel type	PBMR	Variant 1	Variant 2	Variant 3
$k_{\text{eff}}$ at 300 K	1.356	1.348	1.364	1.352
$k_{\text{eff}}$ at 1800 K	1.273	1.281	1.295	1.281
$CT_G$ [pcm/K]	-3.23	-2.61	-2.60	-3.74

Table 11: Criticality vs. graphite temperature and  $CT_G$

Table 10 and Table 11 show that fuel changes introduced in this study lessen the effects of temperature on reactivity change. This leads to somewhat decreased margins on decay heat removal due to a slower reactor shut-down. Since the initial target of the wallpaper fuel was to reduce particle temperature – an effect which is not taken into account here – further investigations were conducted using PANTHERMIX.

## THERMAL-HYDRAULIC AND SAFETY ANALYSIS

### Determination of the thermal profile through pebbles

Due to the fuel geometry and heat transfer, a temperature gradient occurs between particles placed in the centre of the pebble and those at the periphery. This gradient, which is mainly dependent on the power density, can reach up to 200 K at the beginning of life, as shown in [16].

The gradient can be determined, according to [17], by the calculation of heat transfer through successive concentric layers (see Figure 3), defined by the following equation:

$$T_{k+1} = T_k - \frac{Q_{k+1}}{4 * \pi * \lambda_k} * \left( \frac{r_{k+1} - r_k}{r_k * r_{k+1}} \right)$$

where  $T_k$  is the temperature in the shell determined by radius  $r_k$ ,  $Q_{k+1}$  is the power transferred from layer  $k+1$  to layer  $k$ , and  $\lambda$  represents the thermal conductivity of layer  $k$ .

Since fission power is mostly generated locally by kinetic energy release of fission fragments, most of the power generation is concentrated in the fuel zone. But other contributions, with a wider range such as energy deposited due to the slowing down of neutrons or gamma rays, result in power also being produced in

the graphite zones. Generally, around 87.5% of the fission power is deposited in the fuel particles and the rest is averaged over the whole pebble. For this reason, two or three zones need to be defined for the determination of the heat transfer characteristics:

1. The outer fuel-free zone, from  $r = r_{\text{Pebble}}$  to  $r = r_{\text{FZO}}$
2. The fuel zone, from  $r = r_{\text{FZO}}$  to  $r = 0\text{mm}$  (for PBMR fuel) or to  $r = r_{\text{FZI}}$  (for wallpaper fuel)
3. The central fuel-free zone, from  $r = r_{\text{FZI}}$  to  $r = 0\text{mm}$  for wallpaper fuel

Each of the aforementioned zones is then sub-divided into layers. In layers, the power deposited is the sum of short- and long-range powers. The heat transferred to a layer is then the contribution from all powers deposited within the layer concerned.

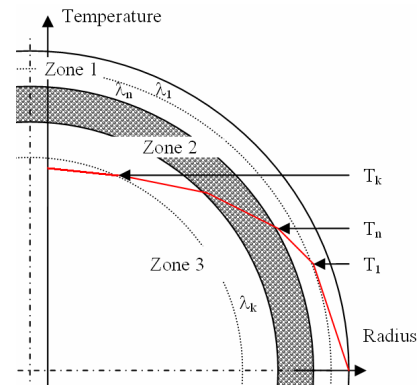


Figure 3: Layer model of the wallpaper pebble

Another key parameter for determining the temperature gradient is graphite thermal conductivity. According to the “Kania” model [18], graphite thermal conductivity depends on the type of graphite, its temperature, heat treatments, neutron fluence and particle packing fraction. To simplify the investigation, the following assumptions were considered:

- The graphite with the highest thermal conductivity is the most relevant, as it would result in the lowest temperature gradients in the pebble. Therefore, the A3-3 type of graphite with thermal treatment at 1950 °C was used throughout this study.
- The influence of temperature was integrated in the calculation by updating the thermal conductivity value for each layer according to its temperature.
- During fuel ageing, the thermal conductivity of graphite drops, which raises the gradients. For a conservative determination of temperature gradient, a neutron fluence of zero was selected.
- Since the thermal conductivity of graphite is an order of magnitude higher than that of  $\text{UO}_2$ , particles are considered as void for the calculation of the integral thermal conductivity. Raising the particle packing fraction decreases the graphite fraction, which lowers the thermal conductivity of the layer. Particle packing fractions equal to 0% (no fuel), 8.95% and 30% are investigated; these represent the fuel free zone, the fuel zone of PBMR pebble and the fuel zone of wallpaper pebbles,

respectively. For wallpaper pebble design, the packing fraction influences the thermal conductivity, but also the central fuel free zone diameter (the number of particles in the pebble is kept constant) and thus the temperature profile across the pebble.

- Finally, since the power density of pebbles changes during burn-up, several assumptions had to be made in order to determine representative temperature profiles: Surface temperature was set to reactor outlet temperature (1 000 °C), while the conservative value of 885 W was selected as the pebble power (pebble power averaged over its lifetime in the reactor).

By summation of all the layers, the temperature profile across the pebble is computed, as shown in Figure 4.

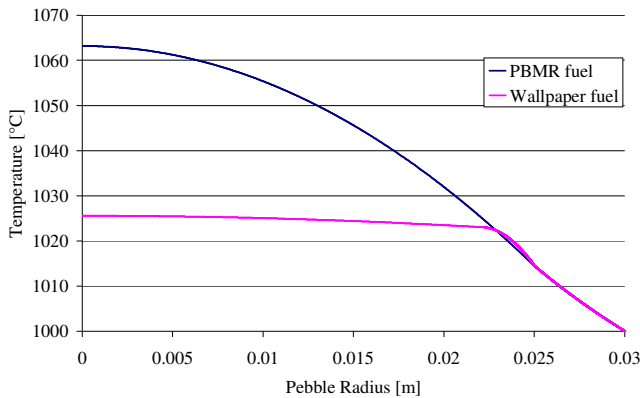


Figure 4: Temperature profile vs. pebble radius

In the case of conventional PBMR fuel, particle temperatures range from 1 014 to 1 063 °C through the fuel zone. For wallpaper fuel, peak temperature and also the range of temperatures in the pebble are smaller: 1 014 to 1 025 °C.

Since fewer particles are positioned in the inner layers of the pebble than in the outer ones, the averaged temperature of particles has to be determined by weighting using the particle volume ratio. This results in an averaged particle temperature of 1 034 °C for conventional PBMR fuel and of 1 020 °C for wallpaper design.

However, the benefits of the decrease of averaged and peak temperatures are accompanied by increased temperature gradients. The averaged temperature increase across the conventional PBMR fuel zone was calculated at 2.92 K/mm, which compares with 3.17 K/mm for the wallpaper design. This may somewhat enhance kernel migration or the amoeba effect [5], which is also responsible for particle failures.

Needless to say, the impacts of parameters (maximum and averaged temperature decrease and amoeba effect) have to be determined experimentally, for instance by means of release measurement under fuel irradiation and post irradiation examinations. It should be noted that temperatures and the increase in temperature within the wallpaper fuel are comparable to those undergone by particles close to the outer edge of the fuel zone of a conventional pebble (cf. Figure 4). Irradiation of conventional pebbles should already provide valuable information concerning the particles' behaviour in wallpaper fuels.

### Fuel cycle with PANTHERMIX

Simulations performed with WIMS, enable the inventory of depleted fuel to be determined. Table 12 presents the atomic density of several Minor Actinides before and after the fuel depletion process. The highest burn-up selected for this study was 90 GWd/t, which corresponds to the “OECD 400MW benchmark” target. Based on the displayed figures, <sup>235</sup>U consumption and different MA production rates can be deduced, as reported in Table 13.

Fuel type	PBMR	Variant 1	Variant 2	Variant 3
<sup>235</sup> U <sub>initial</sub>	1.25E+25	1.25E+25	1.25E+25	1.11E+25
<sup>235</sup> U	4.90E+24	4.87E+24	4.65E+24	4.18E+24
<sup>239</sup> Pu	3.22E+24	3.15E+24	2.62E+24	2.58E+24
<sup>240</sup> Pu	8.78E+23	8.87E+23	8.78E+23	8.90E+23
<sup>241</sup> Pu	9.54E+23	9.35E+23	8.35E+23	8.42E+23
<sup>241</sup> Am	2.99E+22	2.92E+22	2.50E+22	2.53E+22

Table 12: MA atomic density [at.\*m<sup>-3</sup>] at 0 and 90 GWd/t

Fuel type	PBMR	Variant 1	Variant 2	Variant 3
<sup>235</sup> U cons. [g*TW <sub>th</sub> <sup>-1</sup> ]	7.29E+05	7.32E+05	7.55E+05	7.20E+05
<sup>239</sup> Pu prod. [g*TW <sub>th</sub> <sup>-1</sup> ]	3.41E+05	3.33E+05	2.27E+05	2.73E+05
<sup>240</sup> Pu prod. [g*TW <sub>th</sub> <sup>-1</sup> ]	9.33E+04	9.43E+04	9.33E+04	9.46E+04
<sup>241</sup> Pu prod. [g*TW <sub>th</sub> <sup>-1</sup> ]	1.02E+05	9.98E+04	8.91E+04	8.99E+04
<sup>241</sup> Am prod. [g*TW <sub>th</sub> <sup>-1</sup> ]	3.19E+03	3.12E+03	2.67E+03	2.70E+03

Table 13: Evolution of the fuel composition through burn-up

The increases in <sup>235</sup>U consumption (+0.4% and +3.6%) seen in variants 1 and 2 compared to PBMR fuel are due to a reduction of fissile isotope breeding. This also tends to cause a decrease in the production of other MA actinides (-2.3% and -16.4% for <sup>241</sup>Am).

On the other hand, the fall in enrichment introduced by variant 3 tends to lower <sup>235</sup>U consumption (-1.1% compared with PBMR fuel). This decrease is compensated by higher breeding, as suggested by the higher concentration in <sup>240</sup>Pu (+1.4%). Since bred fissile isotopes are subject to fission, the concentration of heavy MA falls, which then lowers the probability of heavier MA breeding (-15.4% for <sup>241</sup>Am compared with PBMR fuel).

Throughout the fuel ageing process, the code determines the neutron multiplication in an infinite medium at different burn-up. Figure 5 presents the values for the four pebbles.

Based on observation of Figure 5, it can be noted that reactivity increases observed in fresh fuel propagate through the fuel depletion process. This suggests that different steady-state cores should display higher reactivities when filled with wallpaper fuels. Unfortunately, no such study has been performed yet.

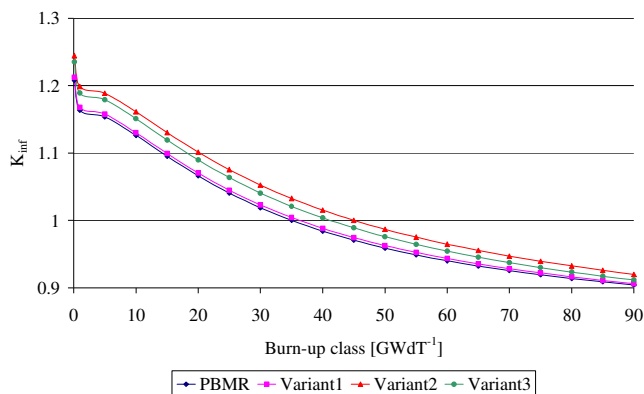


Figure 5: Neutron multiplication in an infinite medium through the fuel ageing process for the four different fuels

### PRODUCTION TECHNOLOGY FOR “WALLPAPER”

In order to be attractive, the wallpaper fuel concept needs to have only a minor impact on the current production process [19]. Fortunately, the additional demands made of the fabrication process are modest and consist in centering different zones: this process is already used for current pebbles, where the graphite shells are moulded around the fuel zone.

Since the resin, used in the 1970s to bind BISO particles for wallpaper design, is no longer needed, the irradiation performance of this fuel is expected to be more favorable and no fabrication issues due to the modification are expected (cf. Figure 6).

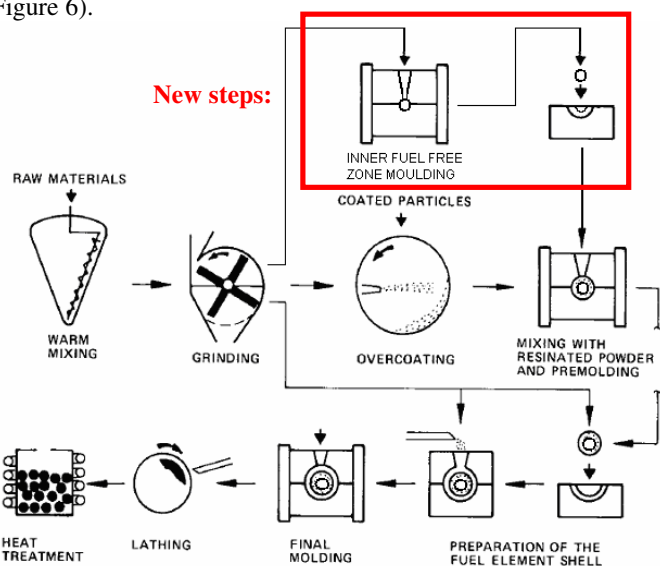


Figure 6: Modification of pebble production

### CONCLUSION

This paper investigates ways of optimizing HTR concept and diversifying its fuel cycle by modifications at fuel element's level. The wallpaper fuel makes it possible to lower the temperature across the pebble. This helps to protect the coating layers and reduces thermal stresses, and the risks of fuel failures resulting in a release of fission products. Wallpaper fuels are

feasible, since the particle packing fraction can be raised significantly, without affecting production, up to 30%. As a result, this newly- created, central fuel-free zone can be used for neutronic optimization of the core. The end result of these optimizations is an increase in neutron multiplication, but these changes also affect spent fuel and nuclear waste composition.

MCNP/MCB simulations have shown that:

- Neutron multiplication of the reactor increases by approx. 1.7%, which is also accompanied by a 7% reduction of MA production (in the case of variant 2);
- Enrichment can be reduced by 6.25% while maintaining neutron multiplication above PBMR design targets (variant 3).

Similar results were calculated by mean of WIMS:

- Simulations performed with variants 1 and 2 show an increase in <sup>235</sup>U consumption (+0.4% and +3.6%) combined with a greater decrease in production of <sup>241</sup>Am (-2.3% and -16.4%).
- The use of variant 3 reduces <sup>235</sup>U consumption by 1.1% and <sup>241</sup>Am production by 15.4% compared to PBMR fuel.

Lastly, peak particle temperature is reduced by approx. 40 K (with an average pebble power of 885W). This reduces the thermal stresses within the coating layers as well as the internal pressure. The latter effect is particularly relevant for Pu-based fuels, as they tend to produce He, which contributes to the increase in internal pressure.

The safety features of the reactor are also expected to be improved by the use of higher-density graphite. This should increase thermal inertia and then decrease maximum temperature during a loss-of-forced-cooling accident.

These considerations also influence reactor economy. Fuel manufacturing costs can be reduced through lower enrichment or by achieving higher burn-up (better use of fissile material). The reactivity caused by changing the fuel allows initial enrichment to be decreased or, alternatively, enables higher burn-up to be achieved.

The fuel cycle might have an even greater impact on fuel economy. Indeed, fuel burning is enhanced by variants 1 and 2 of the wallpaper fuel (a central fuel-free zone filled with matrix or high density graphite) developed in this study, in comparison to breeding and MA production. This reduces MA build-up (less waste) and also reduces proliferation issues around enrichment.

Finally, reducing fuel temperatures and improving the burning capabilities of HTRs would make safer and more efficient plutonium and MA management with HTR, by also improving the sustainability of the concept.

The suggested fuel designs would require irradiation testing for qualification purposes. Since the reactor design stays as it is, this is not part of the critical path for reactor licensing.

This study has shown that there is potential to improve HTR by means of minor modifications to the fuel. Furthermore, understanding physical phenomena makes it possible to investigate different fuel and core geometries in order to further improve neutron economy and to gear the reactor towards higher burning or breeding capabilities, thereby enhancing the sustainability of this very promising reactor concept.

## REFERENCES

- [1] Bäumer, R. et al., AVR: experimental high temperature reactor; 21 years of successful operation for a future energy technology, Association of German engineers (VDI) – Düsseldorf: VDI-Verl., 1990, ISBN 3-18-401015-5.
- [2] <http://www.raphael-project.org/>
- [3] <http://www.puma-project.eu/>
- [4] Teuchert, E., Rütten, H.J., Core physics and fuel cycles of the pebble bed reactor, Nucl. Eng. Des. 34 (1975) 109-118.
- [5] Petti, D.A., Buongiorno, J., Maki, J.T., Hobbins, R.R., Miller, G.K., Key differences in the fabrication, irradiation and high temperature accident testing of US and German TRISO-coated particle fuel, Nuclear Engineering and Design 222 (2003) 281–297.
- [6] Sawa, K., Suzuki, S., Shiozawa, S., Safety criteria and quality control of HTTR fuel, Nuclear Engineering and Design 208 (2001) 305–313.
- [7] Hoenig; Clarence L. (Livermore, CA), United States Patent, 5336520.
- [8] Cetnar, J., Gudowski, W., Wallenius, J., User Manual for Monte-Carlo Continuous Energy Burnup (MCB) Code, Version 1C.
- [9] Briesmeister, J. F., MCNP-A General Monte Carlo N-Particle Transport Code, LA-13709-M, version 4C, 18.12.2000.
- [10] de Haas, J.B.M., Kuiper J.C., and Oppe, J., HTR core physics and transient analyses by the Panthermix code system, MC proceedings, Avignon, France, September 12-15, 2005.
- [11] Reitsma, F., et. al., The OECD/NEA/NSC PBMR Coupled Neutronic/Thermal Hydraulics Transient Benchmark: The PBMR-400 Core Design, Proceedings PHYSOR-2006, Vancouver Canada, 10-14 September 2006.
- [12] Duderstadt, J. J., Hamilton, L. J., Nuclear Reactor Analysis, John Wiley & Sons, Inc. ISBN 0-471-22363-8, 1976.
- [13] Von Halban, H. H., Joliot, J.-F., Kowarsky, L., Improvement in and relating to the liberation of atomic energy, United Kingdom Patent GB633,339, 12 December 1949.
- [14] Kloosterman, J.L., Ougouag, A.M., Comparison and Extension of Dancoff Factors for Pebble-Bed Reactors, Nuclear Science and Engineering, 157:16-29, 2007.
- [15] Hu, S., Wang, R., Gao, Z., Transients tests on blower trip and rod removal at the HTR-10, Nuclear Engineering and Design 236 (2006) 677–680.
- [16] S. de Groot, et al., Modeling of the HFR-EU1BIS experiment and thermomechanical evaluation, Nucl Eng Des (2008).
- [17] VDI- Wärmeatlas Berechnungsblätter für den Wärmeübergang, VDI-Gesellschaft, ISBN 3-18-401048-8, 6. erweiterte Auflage, 1991.
- [18] Kania, M.J., Nickel, H., 1980, Performance assessment of the (Th,U)O<sub>2</sub> HTI-BISO coated particle under PNP/HHT irradiation conditions, KFA Jülich report Jül-1685, ISSN 0366-0885.
- [19] Nickel, H., HTR coated particles and fuel elements, High Temperature Reactor School CEA Cadarache, France (November 4-8, 2002).